SUPPORTING INFORMATION

Theoretical prediction and synthesis of a family of atomic laminate metal borides with in-plane chemical ordering

Martin Dahlqvist,* Quanzheng Tao, Jie Zhou, Justinas Palisaitis, Per O.Å. Persson, Johanna Rosen*

Thin Film Physics, Department of Physics, Chemistry and Biology (IFM), Linköping University, SE-581 83 Linköping, Sweden

* corresponding authors: martin.dahlqvist@liu.se, johanna.rosen@liu.se

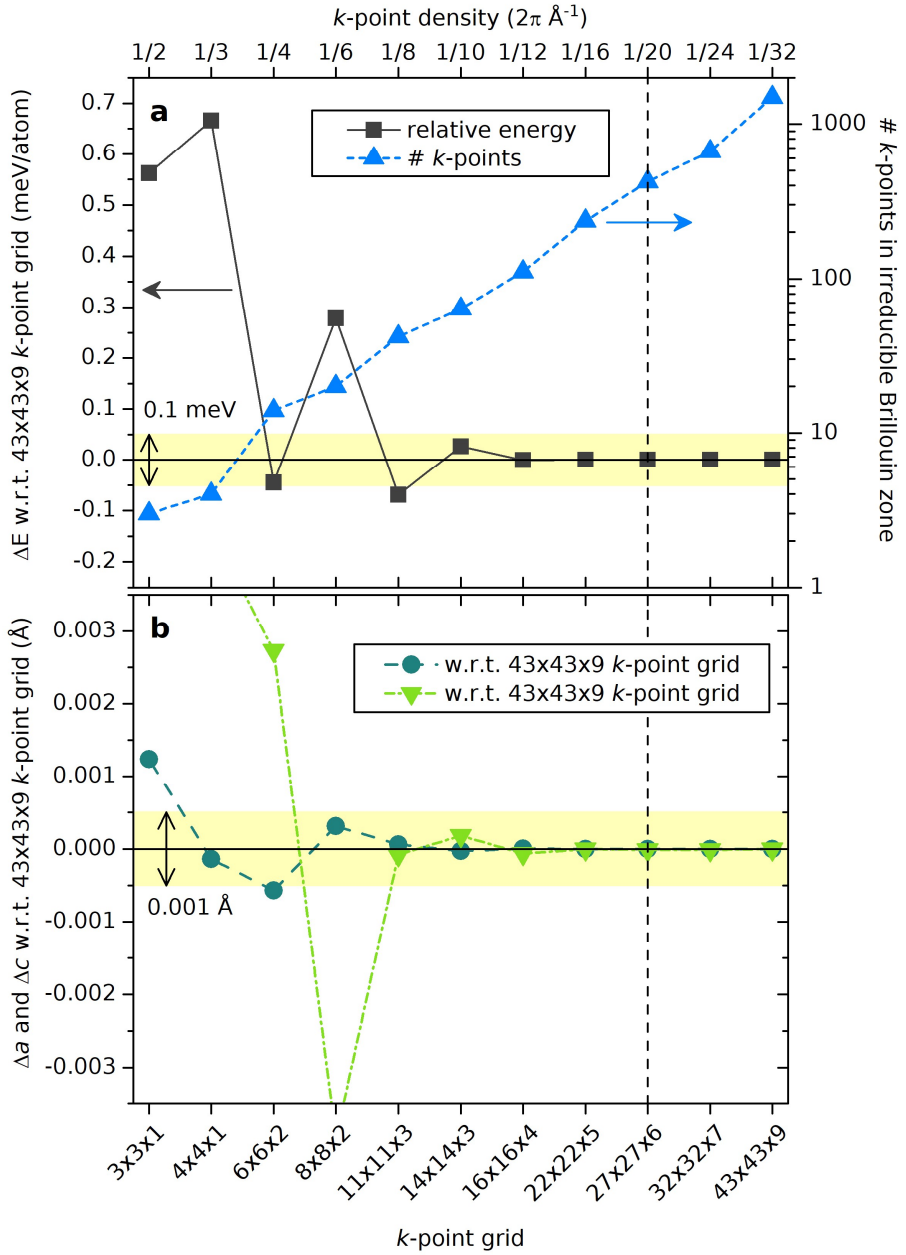

Figure S1. Convergence of relative (a) energy and (b) lattice parameters a and c for $Mo_{4/3}Y_{2/3}AlB_2$ ($R\bar{3}m$) as compared to largest k-point grid (43x43x9) considered as function of k-point grid. Dashed vertical line indicate the k-point density used in this work. Convergence with respect to k-point density used in this work is reached as indicated by the yellow area marked in (a) for an energy interval of 0.1 meV/atom and in (b) for a lattice parameter interval of 0.001 Å.

Table S1. Calculated formation enthalpy ΔH_{cp} for M_2AlB_2 with *Cmmm* and $P\bar{6}m2$ symmetry (in meV/atom) along with identified equilibrium simplex. Experimentally known M_2AlB_2 phases are marked in bold.

M	$\Delta H_{cp}[Cmmm]$ (meV/atom)	$\Delta H_{cp}[P\bar{6}m2]$ (meV/atom)	Equilibrium simplex
Sc	42	88	ScB_2, ScAl
Y	59	131	YB_2, Y_2Al, YAl_2
Ti	26	14	TiAl, TiB_2
Zr	73	63	ZrB_2, Zr_2Al3, $Zr4Al_3$
Hf	77	35	HfB_2, $HfAl_2$, Hf_4Al_3
V	102	73	V_5B_6, VAl_3
Nb	143	56	NbB, Nb_3B_4, $NbAl_3$
Ta	190	75	TaB, Ta_3B_4, $TaAl_3$
Cr	**-13**	118	CrAlB, Cr_4AlB_4
Mo	18	98	MoAlB, Mo_4AlB_4
W	52	143	WAlB, WB
Mn	**-67**	82	MnB, MnB_4, Mn_4Al_{11}
Fe	**-78**	4	FeAlB, FeB
Co	55	120	CoB, B, CoAl

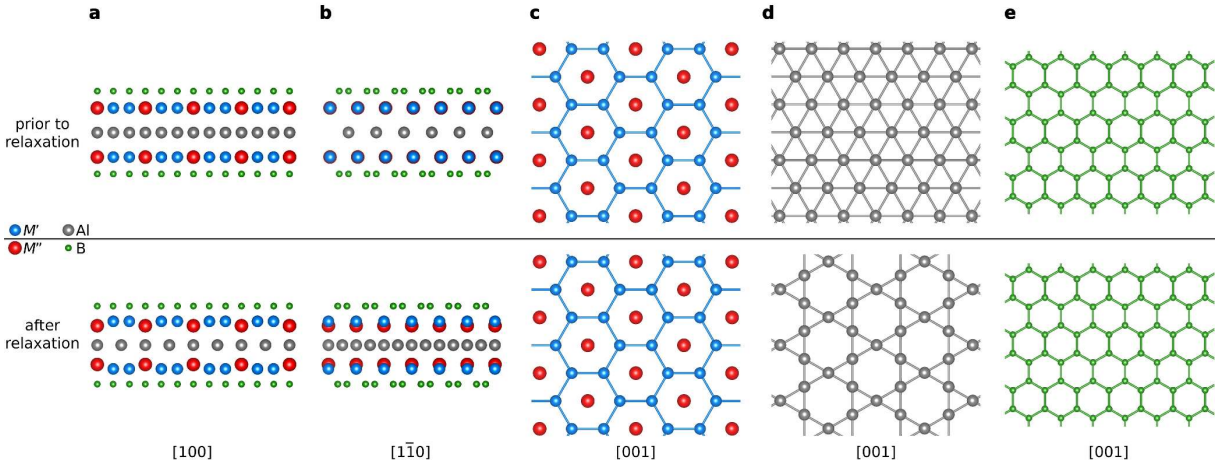

Figure S2. Schematic comparison of the crystal structure of $M'_{4/3}M''_{2/3}AlB_2$ assuming in-plane ordered $P\bar{6}2m$/ $P\bar{6}2c$/ $R\bar{3}m$/$C2$ symmetry, prior to (upper part) and after (lower part) relaxation. A B-*M*-Al-*M*-B section shown along (a) [100] and (b) [1$\bar{1}$0] zone axis. Top view of (c) *M*-layer, (d) Al-layer, and (e) boron layer along [001] zone axis.

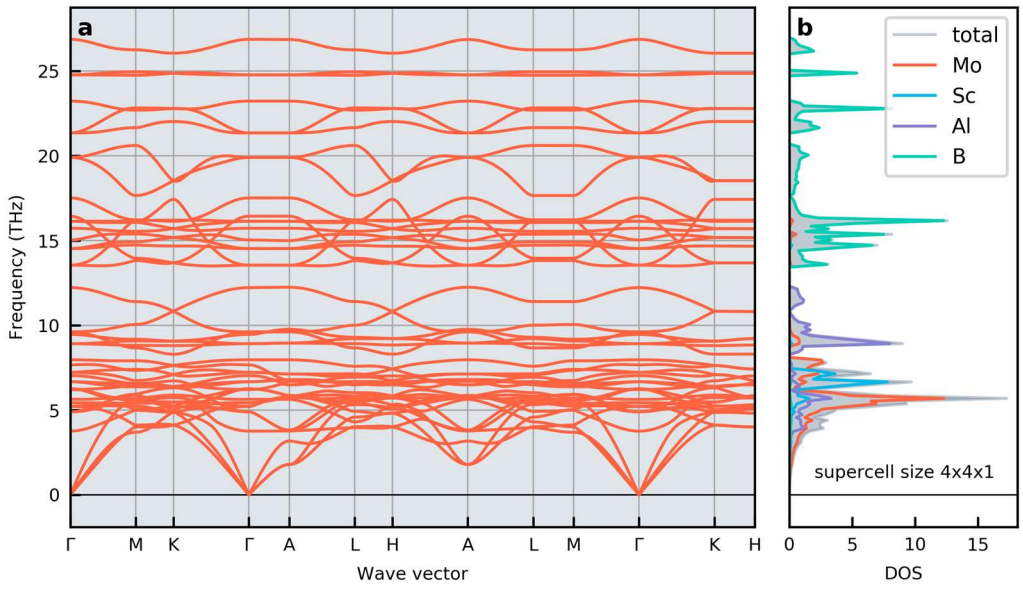

Figure S3. Phonon dispersion and phonon DOS for $Mo_{4/3}Sc_{2/3}AlB_2$ with $P\bar{6}2m$ symmetry (space group 189).

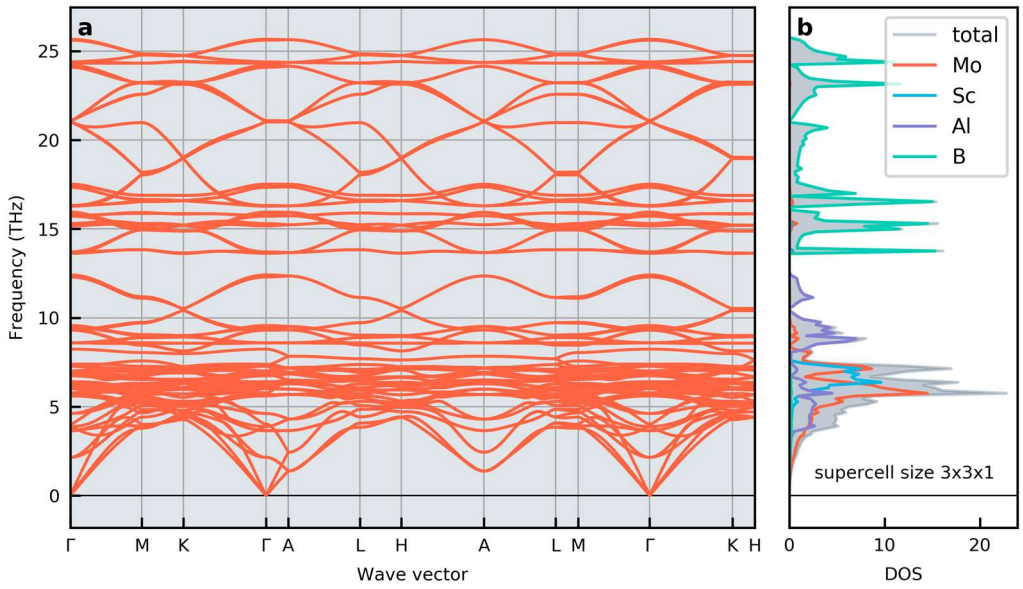

Figure S4. Phonon dispersion and phonon DOS for $Mo_{4/3}Sc_{2/3}AlB_2$ with $P\bar{6}2c$ symmetry (space group 190).

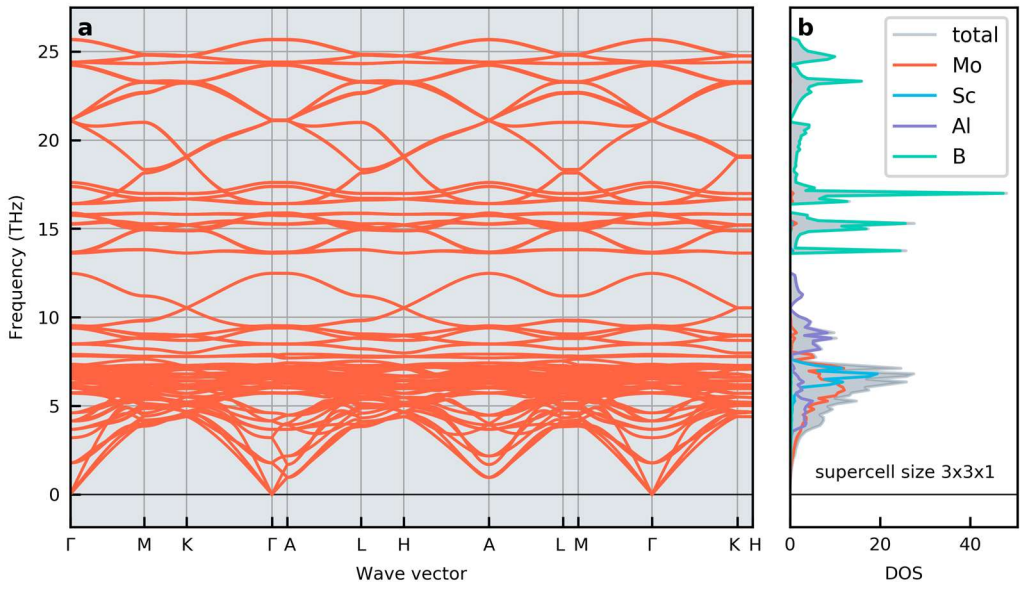

Figure S5. Phonon dispersion and phonon DOS for $Mo_{4/3}Sc_{2/3}AlB_2$ with $R\bar{3}m$ symmetry (space group 166).

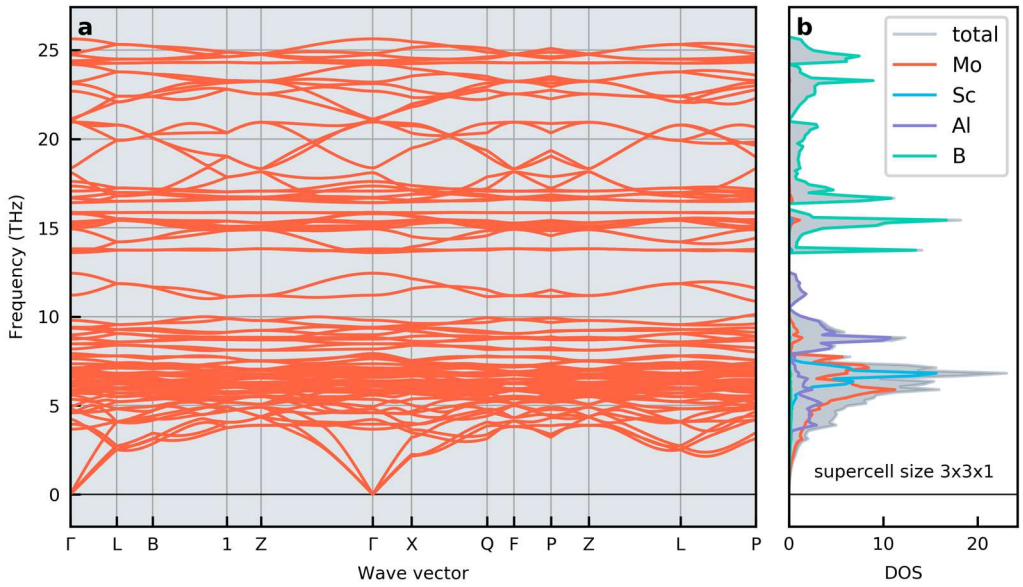

Figure S6. Phonon dispersion and phonon DOS for $Mo_{4/3}Sc_{2/3}AlB_2$ with $C2$ symmetry (space group 5).

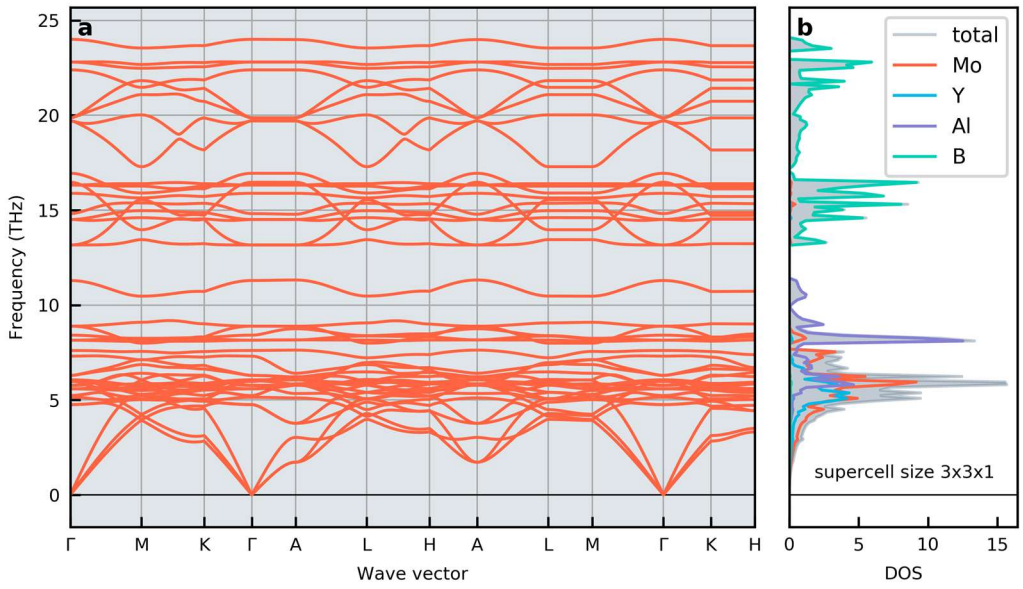

Figure S7. Phonon dispersion and phonon DOS for $Mo_{4/3}Y_{2/3}AlB_2$ with $P\bar{6}2m$ symmetry (space group 189).

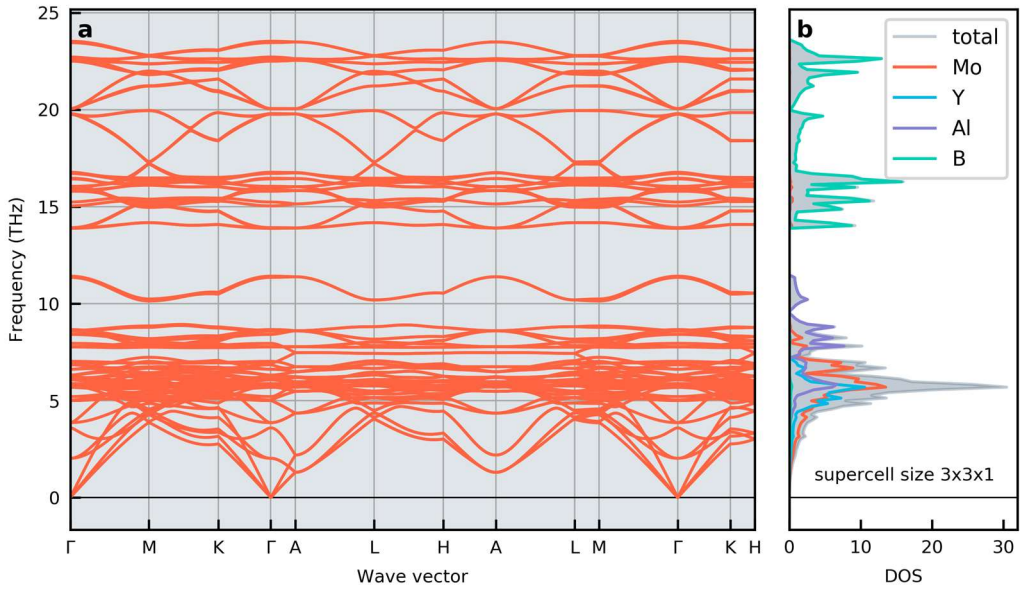

Figure S8. Phonon dispersion and phonon DOS for $Mo_{4/3}Y_{2/3}AlB_2$ with $P\bar{6}2c$ symmetry (space group 190).

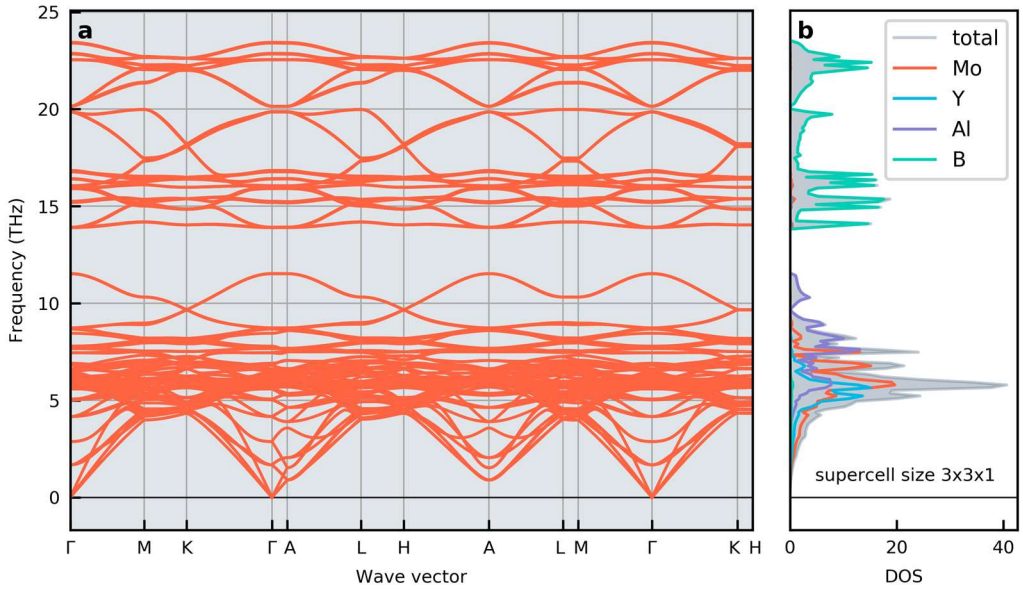

Figure S9. Phonon dispersion and phonon DOS for $Mo_{4/3}Y_{2/3}AlB_2$ with $R\bar{3}m$ symmetry (space group 166).

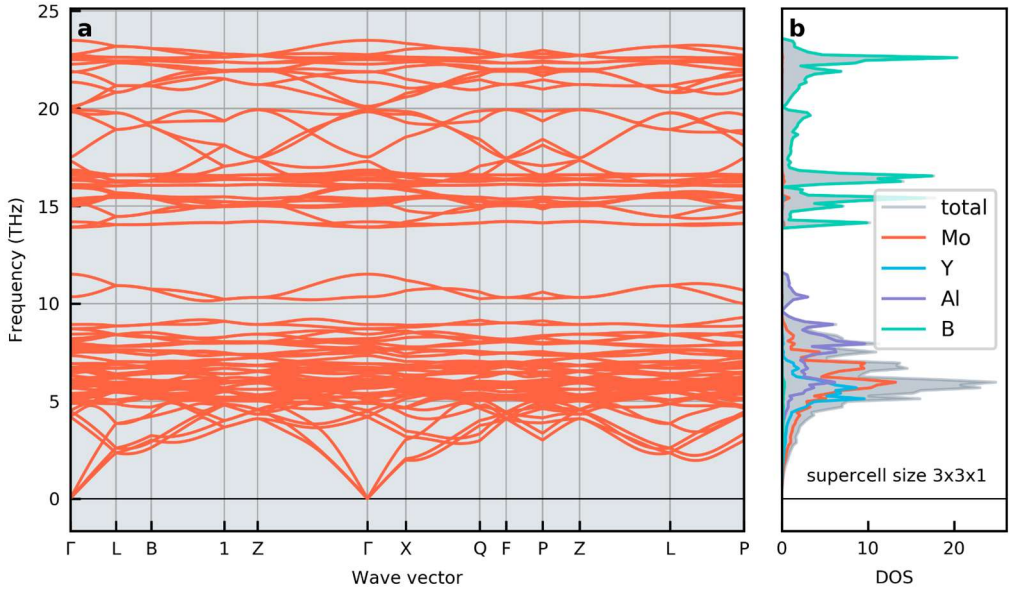

Figure S20. Phonon dispersion and phonon DOS for $Mo_{4/3}Y_{2/3}AlB_2$ with $C2$ symmetry (space group 5).

Table S2. Identified equilibrium simplex for *M′*:*M′′*:Al:B of a 4:2:3:6 composition.

M′	*M′′*	Equilibrium simplex
Sc	Y	ScB_2, YAl_2, Y_2Al, Sc_2Al
Sc	Ti	ScAl, TiB_2, ScB_2
Sc	Zr	ScAl, ZrB_2, ScB_2
Sc	Hf	ScAl, HfB_2, ScB_2
Sc	V	VB, ScB_2, ScAl, $ScAl_2$
Sc	Nb	NbB, ScB_2, ScAl, $ScAl_2$
Sc	Ta	TaB, ScB_2, ScAl, $ScAl_2$
Sc	Cr	ScB_2, $ScAl_2$, Cr_2B
Sc	Mo	ScB_2, $ScAl_2$, Mo_3Al, Mo_3Al_8
Sc	W	ScB_2, W, $ScAl_3$
Sc	Mn	ScB_2, $ScAl_2$, Mn_2B
Sc	Fe	ScB_2, FeAl, ScAl
Sc	Co	ScB_2, CoAl, ScAl
Y	Sc	ScB_2, YB_2, Y_2Al, YAl_2
Y	Ti	TiB_2, YB_2, Y_2Al, YAl_2
Y	Zr	ZrB_2, YB_2, Y_2Al, YAl_2
Y	Hf	HfB_2, YB_2, Y_2Al, YAl_2
Y	V	YB_2, VB, YAl_2, Y_2Al
Y	Nb	YB_2, NbB, YAl_2, Y_2Al
Y	Ta	TaB, YB_2, YAl_2, Y_2Al
Y	Cr	YB_2, CrB, YAl_2, Y_2Al
Y	Mo	MoB, YB_2, YAl_2, Y_2Al
Y	W	YB_2, YAl_2, W_2B
Y	Mn	YB_2, YAl_2, Mn_2B
Y	Fe	YB_2, YAl_2, Fe_2B
Y	Co	YB_2, CoAl, Y_2Al, YAl_2
Ti	Sc	TiB_2, ScAl, TiAl
Ti	Y	YAl_2, TiB_2, Ti_3B4, Y_2Al
Ti	Zr	TiB_2, Ti_3B_4, Zr_2Al_3
Ti	Hf	TiB_2, TiAl, Hf_4Al_3, $HfAl_2$
Ti	V	TiB_2, VB, TiAl, $TiAl_2$
Ti	Nb	TiB_2, TiAl, Nb_2Al, $NbAl_3$
Ti	Ta	TiB_2, TaB, TiAl, $TiAl_2$
Ti	Cr	TiB_2, $TiAl_2$, Cr_2Al
Ti	Mo	TiB_2, $TiAl_2$, Mo_3Al, Mo_3Al_8
Ti	W	TiB_2, W, $TiAl_3$
Ti	Mn	TiB_2, MnAl, $TiAl_2$, $TiMn_2$
Ti	Fe	TiB_2, $TiFe_2Al$, $TiAl_3$, Fe_5Al_8
Ti	Co	TiB_2, CoAl, $TiAl_2$, $TiCo_2Al$
Zr	Sc	ZrB_2, ScAl, Zr_4Al_3, Zr_2Al_3
Zr	Y	ZrB_2, YAl_2, Y_2Al, Zr_4Al_3
Zr	Ti	TiB_2, ZrB_2, Zr_4Al_3, Zr_2Al_3
Zr	Hf	HfB_2, ZrB_2, Zr_4Al_3, Zr_2Al_3
Zr	V	ZrB_2, VB, Zr_2Al_3
Zr	Nb	ZrB_2, NbB, Zr_2Al_3
Zr	Ta	ZrB_2, TaB, Zr_2Al_3
Zr	Cr	ZrB_2, $ZrAl_2$, Cr_2B
Zr	Mo	ZrB_2, $ZrAl_2$, Mo_3Al, Mo_3Al_8
Zr	W	ZrB_2, W, $ZrAl_3$
Zr	Mn	ZrB_2, $ZrAl_2$, Mn_7Al_3, MnAl
Zr	Fe	ZrB_2, $ZrAl_2$, Fe_3Al, FeAl
Zr	Co	ZrB_2, CoAl, Zr_4Al_3, Zr_2Al_3
Hf	Sc	HfB_2, ScAl, $ScAl_2$, Hf_4Al_3
Hf	Y	HfB_2, YAl_2, Y_2Al, Hf_4Al_3
Hf	Ti	TiB_2, HfB_2, Hf_4Al_3, $HfAl_2$
Hf	Zr	HfB_2, Zr_2Al_3, Zr_4Al_3, Hf_4Al_3
Hf	V	VB, HfB_2, $HfAl_2$, Hf_4Al_3
Hf	Nb	HfB_2, $HfAl_2$, Nb_2Al
Hf	Ta	TaB, HfB_2, $HfAl_2$, Hf_4Al_3
Hf	Cr	HfB_2, $HfAl_2$, Cr_2Al
Hf	Mo	HfB_2, $HfAl_2$, Mo_3Al, Mo_3Al_8
Hf	W	HfB_2, W, $HfAl_3$
Hf	Mn	HfB_2, $HfAl_2$, Mn_7Al_3, MnAl
Hf	Fe	HfB_2, FeAl, Hf_4Al_3, $HfAl_2$
Hf	Co	HfB_2, CoAl, Hf_4Al_3, $HfAl_2$
V	Sc	VB, $ScAl_3$, ScB_2
V	Y	YAl_2, YB_2, V_3B_4, V_5B6
V	Ti	VB, $TiAl_3$, TiB_2
V	Zr	VB, $ZrAl_3$, ZrB_2
V	Hf	VB, $HfAl_3$, HfB_2
V	Nb	$NbAl_3$, V_5B_6, VB, Nb_3B_4
V	Ta	TaB, $TaAl_3$, V_3B_4, V_5B_6
V	Cr	Cr_2AlB_2, V_5B_6, VAl_3
V	Mo	MoAlB, VB, V_5B_6, Mo_3Al_8
V	W	WB, VB, WAl_5, V_5B_6
V	Mn	V_5B_6, Mn_2AlB_2, Mn_4Al_{11}, V_3B_4
V	Fe	V_2B_3, V_3B_4, Fe_5Al_8, Fe_2AlB_2
V	Co	V_2B_3, CoAl, Co_2Al_5
Nb	Sc	NbB, $ScAl_3$, ScB_2
Nb	Y	YAl_2, NbB, Nb_3B_4, YB_2,
Nb	Ti	NbB, TiB_2, $NbAl_3$, Nb_2Al
Nb	Zr	NbB, ZrB_2, $ZrAl_2$, $NbAl_3$
Nb	Hf	HfB_2, NbB, $NbAl_3$, Nb_2Al
Nb	V	VB, $NbAl_3$, Nb_3B_4
Nb	Ta	TaB, $NbAl_3$, Nb_3B_4
Nb	Cr	CrB, Nb_3B_4, $NbAl_3$
Nb	Mo	Nb_3B_4, MoB, NbB, Mo_3Al_8
Nb	W	WB, Nb_3B_4, $NbAl_3$
Nb	Mn	NbB, Mn_2AlB_2, $NbAl_3$, Nb_3B_4
Nb	Fe	FeAl, Nb_2B_3, NbB_2, $NbAl_3$
Nb	Co	Nb_2B_3, CoAl, Co_2Al_5
Ta	Sc	TaB, ScB_2, $ScAl_3$
Ta	Y	TaB, YAl_2, YB_4
Ta	Ti	TaB, TiB_2, $TiAl_3$
Ta	Zr	TaB, ZrB_2, $ZrAl_3$
Ta	Hf	TaB, HfB_2, $HfAl_3$
Ta	V	TaB, $TaAl_3$, V_2B_3
Ta	Nb	TaB, $NbAl_3$, Nb_2B_3, Ta_3B_4
Ta	Cr	TaB, Cr_2AlB_2, Ta_3B_4, $TaAl_3$
Ta	Mo	TaB, MoAlB, Ta_3B_4, Mo_3Al_8
Ta	W	TaB, WAlB, WAl_5, Ta_3B_4
Ta	Mn	TaB, Ta_3B_4, Mn_2AlB_2, Mn_4Al_{11}
Ta	Fe	Ta_3B_4, TaB_2, Fe_5Al_8, Fe_2AlB_2
Ta	Co	CoAl, TaB_2, Ta_3B_4, Co_2Al_5
Cr	Sc	CrB, $ScAl_3$, ScB_2
Cr	Y	CrB, YAl_2, YB_4
Cr	Ti	TiB_2, Cr_2AlB_2, Cr_2Al, $TiAl_3$
Cr	Zr	CrB, $ZrAl_3$, ZrB_2
Cr	Hf	HfB_2, Cr_2AlB_2, Cr_2Al, $HfAl_3$
Cr	V	Cr_2AlB_2, VAl_3, V_5B_6
Cr	Nb	Cr_2AlB_2, CrB, Nb_3B_4, $NbAl_3$
Cr	Ta	Cr_2AlB_2, TaB, Ta_3B_4, $TaAl_3$
Cr	Mo	MoAlB, CrB, Cr_2AlB_2
Cr	W	Cr_2AlB_2, WB, WAlB
Cr	Mn	Cr_2AlB_2, Mn_2AlB_2
Cr	Fe	Cr_2AlB_2, Fe_2AlB_2
Cr	Co	CrB_2, CrB, CoAl, Co_2Al_5
Mo	Sc	MoB, ScB_2, Mo_3Al_8, Mo_3Al
Mo	Y	MoB, YAl_2, YB_4
Mo	Ti	MoB, TiB_2, Mo_3Al_8, Mo_3Al
Mo	Zr	ZrB_2, MoB, Mo_3Al_8, Mo_3Al
Mo	Hf	HfB_2, MoB, Mo_3Al_8, Mo_3Al
Mo	V	MoAlB, VB, MoB
Mo	Nb	MoB, MoAlB, Nb_3B_4, Mo_3Al_8
Mo	Ta	MoAlB, TaB, Mo_4AlB_4
Mo	Cr	MoAlB, CrB, MoB
Mo	W	MoAlB, WB, MoB
Mo	Mn	MoAlB, MoB, Mn_2AlB_2
Mo	Fe	MoAlB, MoB, Fe_2AlB_2
Mo	Co	CoAl, MoB_2, MoB, MoAlB
W	Sc	WB, $ScAl_3$, ScB_2
W	Y	WB, YAl_2, YB_4
W	Ti	TiB_2, W_2B, WB, WAl_5
W	Zr	ZrB_2, W_2B, WB, WAl_5
W	Hf	HfB_2, W_2B, WB, WAl_5
W	V	WB, WAl_5, V_3B_4, V_5B_6
W	Nb	WB, WAlB, $NbAl_3$, Nb_2B_3
W	Ta	WAlB, TaB, WB
W	Cr	WB, WAlB, Cr_2AlB_2
W	Mo	WB, MoAlB, WAlB
W	Mn	WB, WAlB, Mn_2AlB_2
W	Fe	WAlB, WB, Fe_2AlB_2
W	Co	WB_2, WB, CoAl, Co_2Al_5
Mn	Sc	MnAl, ScB_2, Mn_2AlB_2
Mn	Y	MnB, YAl_2, YB_4
Mn	Ti	MnAl, TiB_2, Mn_2AlB_2
Mn	Zr	MnAl, ZrB_2, Mn_2AlB_2
Mn	Hf	MnAl, HfB_2, Mn_2AlB_2
Mn	V	Mn_2AlB_2, V_5B_6, V_3B_4, Mn_4Al_{11}
Mn	Nb	Mn_2AlB_2, NbB, $NbAl_3$, Nb_3B_4
Mn	Ta	Mn_2AlB_2, TaB, Ta_3B_4, Mn_4Al_{11}
Mn	Cr	Mn_2AlB_2, Cr_2AlB_2
Mn	Mo	Mn_2AlB_2, MoAlB, MoB
Mn	W	Mn_2AlB_2, WAlB, WB
Mn	Fe	Mn_2AlB_2, Fe_2AlB_2
Mn	Co	CoAl, MnB, Mn_2AlB_2, MnB_4
Fe	Sc	FeAl, ScB_2, Fe_2AlB_2
Fe	Y	Fe_2B, FeAl,YB_4, YAl_2
Fe	Ti	TiB_2, Fe_2AlB_2, Fe_3Al, Fe_5Al_8
Fe	Zr	FeAl, ZrB_2, Fe_2AlB_2
Fe	Hf	FeAl, HfB_2, Fe_2AlB_2
Fe	V	Fe_2AlB_2, V_2B_3, V_3B_4, Fe_5Al_8
Fe	Nb	FeAl, NbB_2, Fe_2AlB_2
Fe	Ta	Fe_2AlB_2, Ta_3B_4, TaB_2, Fe_5Al_8
Fe	Cr	Fe_2AlB_2, Cr_2AlB_2
Fe	Mo	Fe_2AlB_2, MoAlB, MoB
Fe	W	Fe_2AlB_2, WAlB, WB
Fe	Mn	Fe_2AlB_2, Mn_2AlB_2
Fe	Co	Fe_2AlB_2, CoAl, CoB, B
Co	Sc	CoAl, ScB_2, CoB, $ScB1_2$
Co	Y	CoAl, YB_2, CoB, YB_4
Co	Ti	CoAl, TiB_2, CoB, B
Co	Zr	CoAl, ZrB_2, CoB, B
Co	Hf	CoAl, HfB_2, CoB, B
Co	V	CoAl, VB_2, $VCoB_3$, B
Co	Nb	CoAl, NbB_2, CoB, B
Co	Ta	CoAl, TaB_2, CoB, B
Co	Cr	CoAl, CrB_2, CoB, CrB_4
Co	Mo	CoAl, MoB_2, CoB, B
Co	W	CoAl, CoB, WB_4
Co	Mn	CoAl, CoB, MnB, MnB_4
Co	Fe	CoAl, CoB, B, Fe_2AlB_2

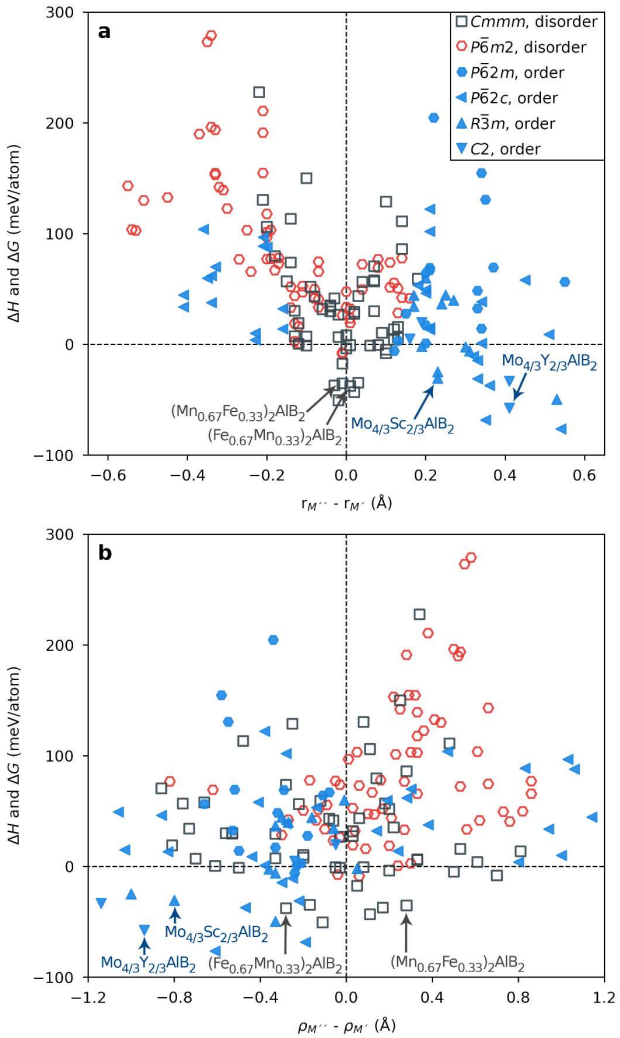

Figure S11. ΔH or ΔG, from Fig. 3b, as function of (a) size and (b) electronegativity difference between M'' and M'. Symbols represent crystal structure and chemical order of lowest energy for a given combination of M' and M''; *Cmmm* with disorder (open squares), $P\bar{6}m2$ with disorder (open hexagon), and in-plane ordered *i*-MAB phases with $P\bar{6}2m$ (filled hexagon), $P\bar{6}2c$ (filled left triangle), $R\bar{3}m$ (filled up triangle) and $C2$ (filled down triangle) symmetries. Experimentally reported phases are marked in both panels.

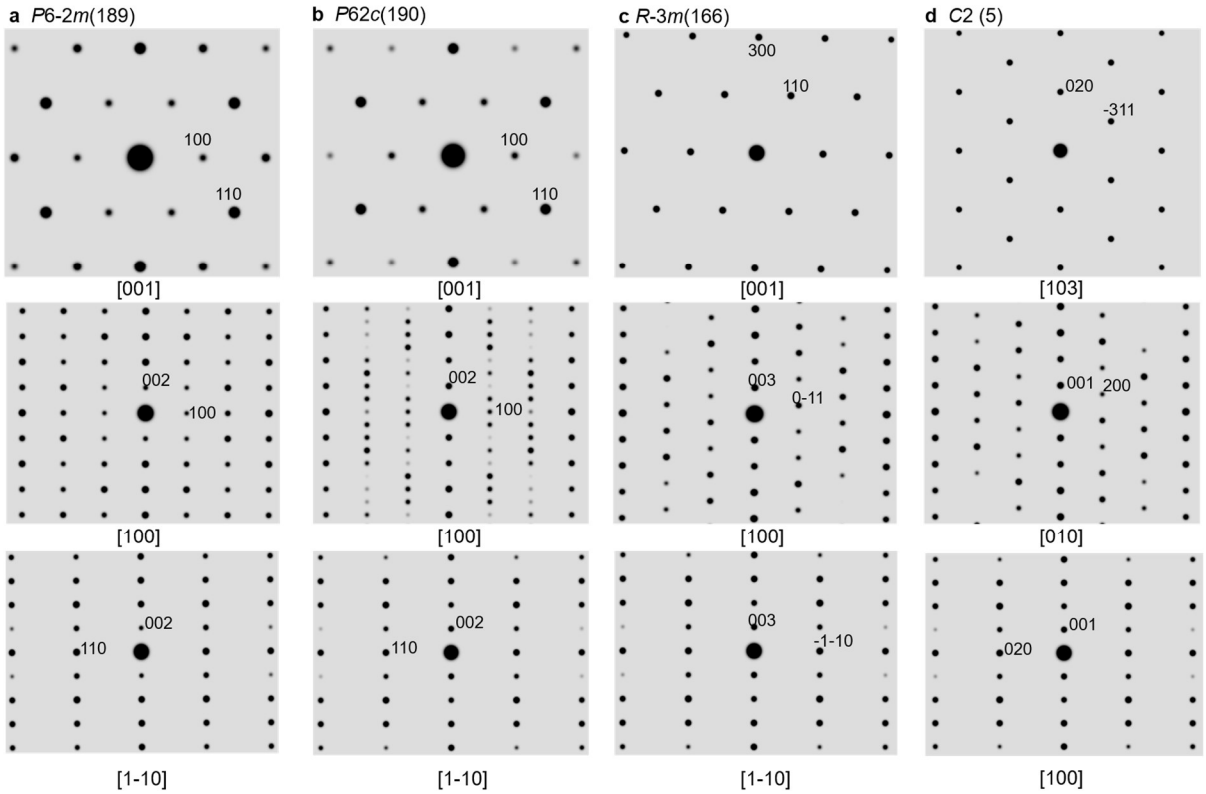

Figure S12. Simulated selective area electron diffraction patterns along [001], [100], and $[1\bar{1}0]$ zone axes for different *i*-MAB polymorphs with (a) $P\bar{6}2m$, (b) $P\bar{6}2c$, (c) $R\bar{3}m$ and (d) $C2$ symmetries.

Table S3. Rietveld refinement of $Mo_{4/3}Y_{2/3}AlB_2$ assuming a hexagonal $R\bar{3}m$ (#166) symmetry. From the Rietveld refinement of the XRD pattern shown in Fig. 4a, the mass fractions of the *i*-MAB phase $Mo_{4/3}Y_{2/3}AlB_2$, MoB and Y_2O_3 were: 80, 15 and 5 wt%, respectively. The total χ^2 value was 3.23.

Formula (unit cell)	$Mo_{12}Y_6Al_9B_{18}$
Space group	$R\bar{3}m$ (#166)
$a = b$(Å)	5.44577(9)
c (Å)	22.69048(38)
$\alpha = \beta$ (°)	90
γ (°)	120
Mo	6c (0.00000, 0.00000, 0.56468(15))
Mo	6c (0.00000, 0.00000, 0.77062(14))
Y	6c (0.00000, 0.00000, -0.07931(17))
Al	9e (0.50000, 0.00000, 0.00000)
B	18g (0.32863(59), 0.00000, 0.00000)

Table S4. Calculated crystallographic data for $Mo_{4/3}Y_{2/3}AlB_2$ using the GGA-PBE exchange-correlation functional with Wyckoff positions given for each unique crystallographic site.

Space group	Lattice parameter (Å)	Atomic position
$P\bar{6}2m$ (189)	a = 5.434	Mo 4h (0.33333, 0.66667, 0.69125)
	c = 7.644	Y 2e (0.00000, 0.00000, 0.23686)
		Al 3f (0.49975, 0.00000, 0.00000)
		B 3g (0.66787, 0.00000, 0.50000)
		B 3g (0.36788, 0.00000, 0.50000)
$P\bar{6}2c$ (190)	a = 5.464	Mo 4f (0.33333, 0.66667, 0.40766)
	c = 15.183	Mo 4e (0.00000, 0.00000, 0.09514)
		Y 4f (0.33333, 0.66667, 0.63022)
		Al 6h (0.66728, 0.83376, 0.25000)
		B 6g (0.66585, 0.00000, 0.00000)
		B 6g (0.33415, 0.00000, 0.00000)
$R\bar{3}m$ (166)	a = 5.465	Mo 6c (0.00000, 0.00000, 0.56355)
	c = 22.755	Mo 6c (0.00000, 0.00000, 0.77221)
		Y 6c (0.00000, 0.00000, -0.07973)
		Al 9e (0.50000, 0.00000, 0.00000)
		B 18g (0.33377, 0.00000, 0.50000)
$C2$ (5)	a = 9.473	Mo 4c (0.27262, 0.33333, 0.81672)
	b = 5.467	Mo 4c (-0.06298, 0.33333, 0.80968)
	c = 8.214	Y 4c (0.57996, 0.33335, 0.73957)
	β = 112.564	Al 2b (0.00000, 0.33346, 0.50000)
		Al 4c (0.75006, 0.08325, 0.50001)
		B 2a (0.00000, -0.00076, 0.00000)
		B 4c (0.66712, 0.00025, 0.00000)
		B 2a (0.00000, 0.66742, 0.00000)
		B 4c (0.16713, 0.16643, 0.00001)

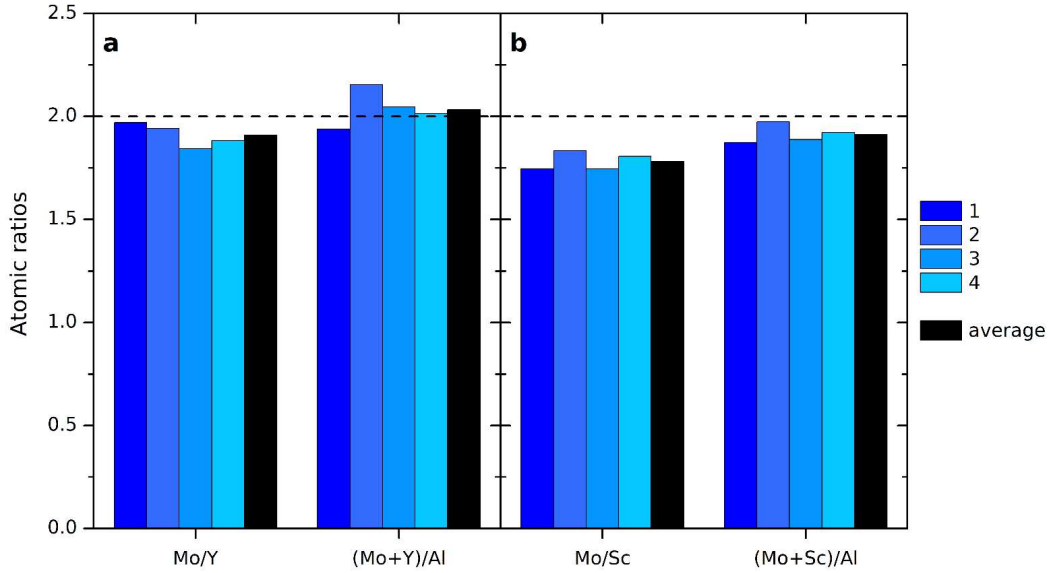

Figure S13. Atomic ratios from four individual powder particles along with average values from EDX for (a) $Mo_{4/3}Y_{2/3}AlB_2$ and (b) $Mo_{4/3}Sc_{2/3}AlB_2$.

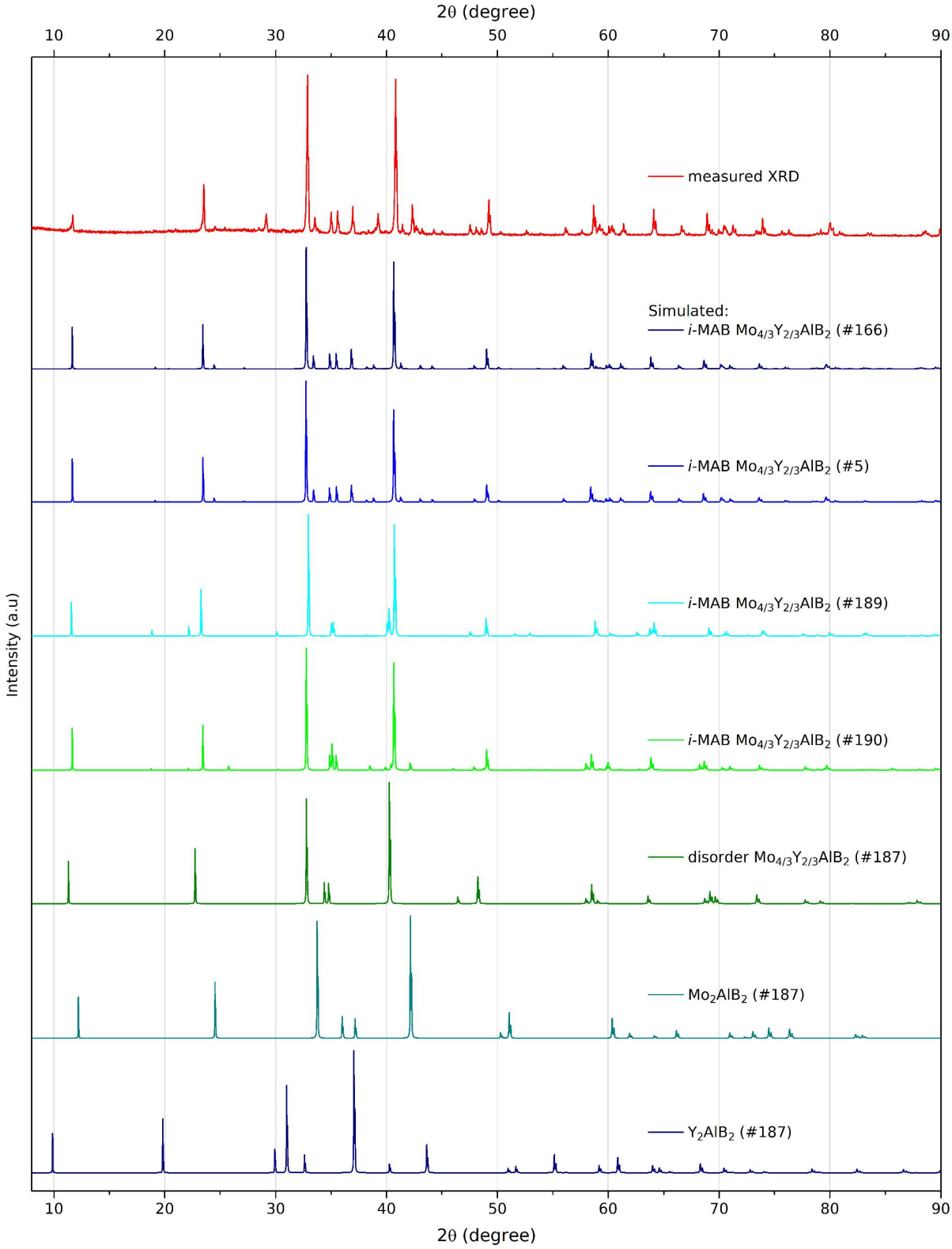

Figure S14. Measured XRD of the $Mo_{4/3}Y_{2/3}AlB_2$ sample along with simulated diffractograms for four *i*-MAB and one disordered $Mo_{4/3}Y_{2/3}AlB_2$. In addition, simulated diffractograms for Mo_2AlB_2 and Y_2AlB_2 with $P\bar{6}m2$ symmetry is shown.

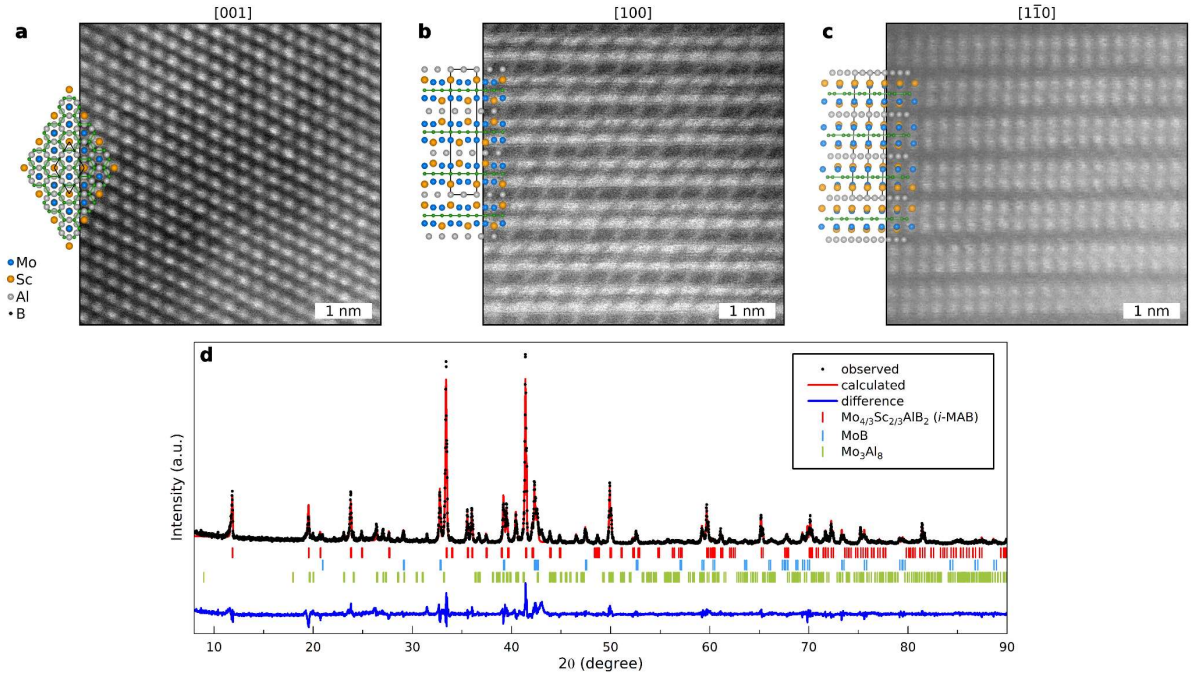

Figure S15. Experimental characterization of synthesized $Mo_{4/3}Sc_{2/3}AlB_2$ *i*-MAB phase. (a-c) In-plane chemical ordering of the *i*-MAB phase is evident from STEM images along the [001], [100] and [1$\bar{1}$0] zone axis, respectively. Schematics to the left of each image represent the corresponding atomic arrangements considering the hexagonal $R\bar{3}m$ (#166) structure. (d) Rietveld refinement of XRD of sample assuming space group $R\bar{3}m$ (#166).

Table S5. Rietveld refinement of $Mo_{4/3}Sc_{2/3}AlB_2$ assuming a hexagonal $R\bar{3}m$ (#166) symmetry. From the Rietveld refinement of the XRD pattern shown in Fig. 5a, the mass fractions of the *i*-MAB phase $Mo_{4/3}Sc_{2/3}AlB_2$, MoB and Mo_3Al_8 were: 62, 20 and 18 wt%, respectively. The total χ^2 value was 3.76.

Formula (unit cell)	$Mo_{12}Sc_6Al_9B_{18}$
Space group	$R\bar{3}m$ (#166)
$a = b$(Å)	5.36261(8)
c (Å)	22.44267(42)
$\alpha = \beta$ (°)	90
γ (°)	120
Mo	6c (0.00000, 0.00000, 0.66543(15))
Mo	6c (0.00000, 0.00000, 0.76785(15))
Y	6c (0.00000, 0.00000, -0.08884(34))
Al	9e (0.50000, 0.00000, 0.00000)
B	18g (0.37120(400), 0.00000, 0.00000)

Table S6. Calculated crystallographic data for $Mo_{4/3}Sc_{2/3}AlB_2$ using the GGA-PBE exchange-correlation functional with Wyckoff positions given for each unique crystallographic site.

Space group	Lattice parameter (Å)	Atomic position
$P\bar{6}2m$ (189)	a = 5.35158	Mo 4h (0.33333, 0.66667, 0.69540)
	c = 7.51226	Sc 2e (0.00000, 0.00000, 0.24794)
		Al 3f (0.49978, 0.00000, 0.00000)
		B 3g (0.67029, 0.00000, 0.50000)
		B 3g (0.32972, 0.00000, 0.50000)
$P\bar{6}2c$ (190)	a = 5.37974	Mo 4f (0.33333, 0.66667, 0.40521)
	c = 14.92960	Mo 4e (0.00000, 0.00000, 0.09690)
		Sc 4f (0.33333, 0.66667, 0.62474)
		Al 6h (0.66692, 0.83284, 0.25000)
		B 6g (0.66487, 0.00000, 0.00000)
		B 6g (0.33513, 0.00000, 0.00000)
$R\bar{3}m$ (166)	a = 5.38270	Mo 6c (0.00000, 0.00000, 0.56457)
	c = 22.38392	Mo 6c (0.00000, 0.00000, 0.77050)
		Sc 6c (0.00000, 0.00000, -0.08331)
		Al 9e (0.50000, 0.00000, 0.00000)
		B 18g (0.33514, 0.00000, 0.50000)
$C2$ (5)	a = 9.32832	Mo 4c (0.27090, 0.33334, 0.81182)
	b = 5.38336	Mo 4c (-0.06397, 0.33334, 0.80649)
	c = 8.08154	Sc 4c 0.58345, 0.33336, 0.75038)
	β = 112.58693	Al 2b (0.00000, 0.33549, 0.50000)
		Al 4c (0.75111, 0.08219, 0.50000)
		B 2a (0.00000, -0.00175, 0.00000)
		B 4c (0.66763, 0.00073, 0.00003)
		B 2a (0.00000, 0.66847, 0.00000)
		B 4c (0.16765, 0.16593, 0.00003)

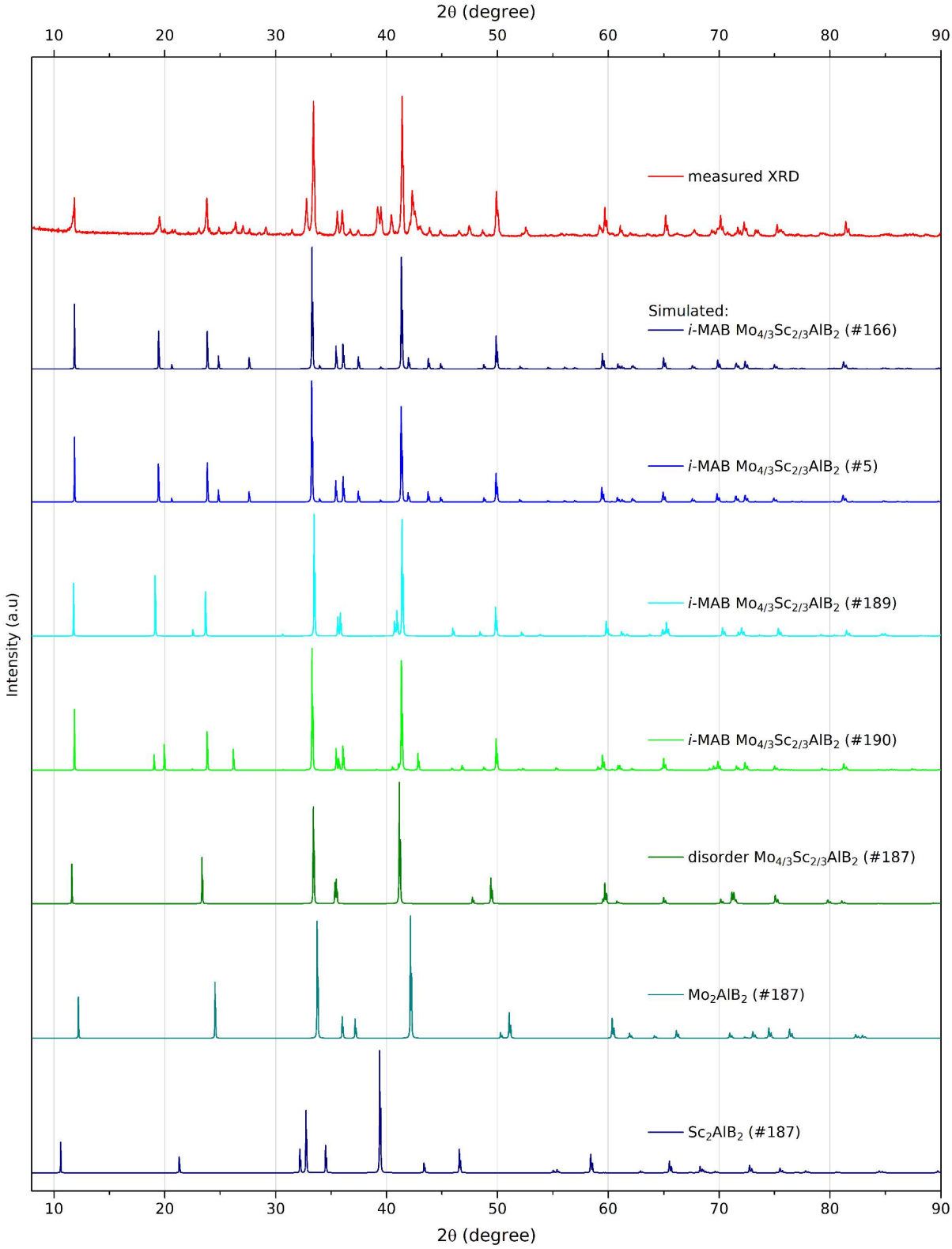

Figure S16. Measured XRD of the $Mo_{4/3}Sc_{2/3}AlB_2$ sample along with simulated diffractograms for four *i*-MAB and one disordered $Mo_{4/3}Sc_{2/3}AlB_2$. In addition, simulated diffractograms for Mo_2AlB_2 and Sc_2AlB_2 with $P\bar{6}m2$ symmetry is shown.

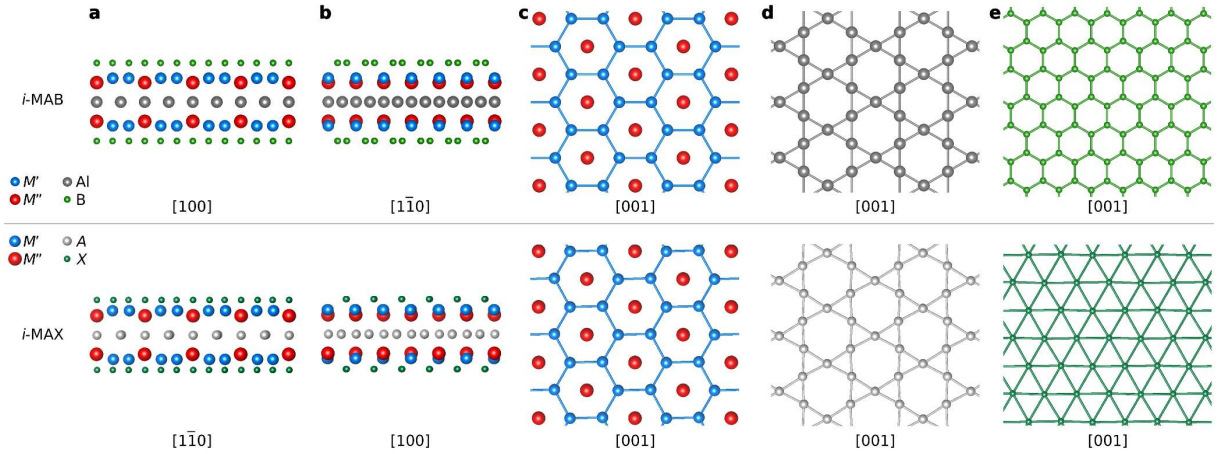

Figure S17. Schematic illustration and comparison of *i*-MAB and *i*-MAX phases locally along (a) [100] and (b) [$1\bar{1}0$] zone axes and for (c) *M*-layer, (d) Al- and *A*-layer, and (e) B and *X*-layer along [001] zone axes.